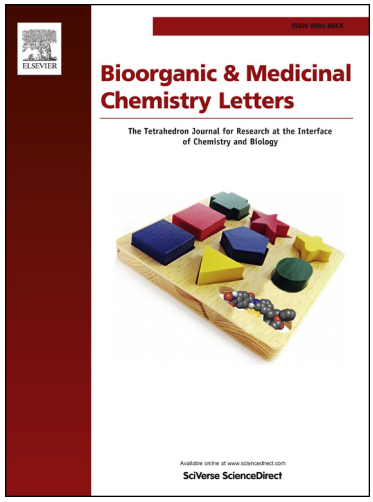

Discovery of 1-(4-(5-(5-Amino-6-(5-*tert*-butyl-1,3,4-oxadiazol-2-yl)pyrazin-2-yl)-1-ethyl-1,2,4-triazol-3-yl)piperidin-1-yl)-3-hydroxypropan-1-one (AZD8835): A Potent and Selective Inhibitor of PI3Kα and PI3Kδ for the Treatment of Cancers

Bernard Barlaam, Sabina Cosulich, Bénédicte Delouvrié, Rebecca Ellston, Martina Fitzek, Hervé Germain, Stephen Green, Urs Hancox, Craig S. Harris, Kevin Hudson, Christine Lambert-van der Brempt, Honorine Lebraud, Françoise Magnien, Maryannick Lamorlette, Antoine Le Griffon, Rémy Morgentin, Gilles Ouvry, Ken Page, Georges Pasquet, Urszula Polanska, Linette Ruston, Twana Saleh, Michel Vautier, Lara Ward

PII: S0960-894X(15)30111-6
DOI: http://dx.doi.org/10.1016/j.bmcl.2015.10.002
Reference: BMCL 23158

To appear in: *Bioorganic & Medicinal Chemistry Letters*

Received Date: 11 September 2015
Revised Date: 30 September 2015
Accepted Date: 1 October 2015

Please cite this article as: Barlaam, B., Cosulich, S., Delouvrié, B., Ellston, R., Fitzek, M., Germain, H., Green, S., Hancox, U., Harris, C.S., Hudson, K., Brempt, C.L-v., Lebraud, H., Magnien, F., Lamorlette, M., Griffon, A.L., Morgentin, R., Ouvry, G., Page, K., Pasquet, G., Polanska, U., Ruston, L., Saleh, T., Vautier, M., Ward, L., Discovery of 1-(4-(5-(5-Amino-6-(5-*tert*-butyl-1,3,4-oxadiazol-2-yl)pyrazin-2-yl)-1-ethyl-1,2,4-triazol-3-yl)piperidin-1-yl)-3-hydroxypropan-1-one (AZD8835): A Potent and Selective Inhibitor of PI3Kα and PI3Kδ for the Treatment of Cancers, *Bioorganic & Medicinal Chemistry Letters* (2015), doi: http://dx.doi.org/10.1016/j.bmcl.2015.10.002

Bioorganic & Medicinal Chemistry Letters
journal homepage: www.elsevier.com

Discovery of 1-(4-(5-(5-Amino-6-(5-*tert*-butyl-1,3,4-oxadiazol-2-yl)pyrazin-2-yl)-1-ethyl-1,2,4-triazol-3-yl)piperidin-1-yl)-3-hydroxypropan-1-one (AZD8835): A Potent and Selective Inhibitor of PI3Kα and PI3Kδ for the Treatment of Cancers

Bernard Barlaam*,[b] Sabina Cosulich,[b] Bénédicte Delouvrié,[a] Rebecca Ellston,[b] Martina Fitzek,[b] Hervé Germain,[a] Stephen Green,[b] Urs Hancox,[b] Craig S. Harris,[a,1] Kevin Hudson,[b] Christine Lambert-van der Brempt,[a] Honorine Lebraud,[a] Françoise Magnien,[a] Maryannick Lamorlette,[a] Antoine Le Griffon,[a] Rémy Morgentin,[a,2] Gilles Ouvry,[a,1] Ken Page,[b] Georges Pasquet,[a] Urszula Polanska,[b] Linette Ruston,[b] Twana Saleh,[a] Michel Vautier,[a] Lara Ward.[b]

[a] *AstraZeneca, Centre de Recherches, Z.I. La Pompelle, B.P. 1050, Chemin de Vrilly, 51689 Reims, Cedex 2, France*
[b] *AstraZeneca, Oncology iMed, Alderley Park, Macclesfield, Cheshire SK10 4TG, United Kingdom*

corresponding author: B.Barlaam e-mail: bernard.barlaam2@astrazeneca.com
[1] *current address: Galderma R&D, les Templiers, 2400 route des Colles, 06410 Sophia-Antipolis, France*
[2] *current address: Edelris, 115 avenue Lacassagne, 69003 Lyon, France*

ARTICLE INFO

Article history:
Received
Revised
Accepted
Available online

Keywords:
PI3Kα
PI3Kδ
Kinase
PIK3CA mutation

ABSTRACT

Starting from potent inhibitors of PI3Kα having poor general kinase selectivity (e.g. **1** and **2**), optimisation of this series led to the identification of **25**, a potent inhibitor of PI3Kα (wild type, E545K and H1047R mutations) and PI3Kδ, selective vs. PI3Kβ and PI3Kγ, with excellent general kinase selectivity. Compound **25** displayed low metabolic turnover and suitable physical properties for oral administration. *In vivo*, compound **25** showed pharmacodynamic modulation of AKT phosphorylation and near complete inhibition of tumour growth (93% tumour growth inhibition) in a murine H1047R PI3Kα mutated SKOV-3 xenograft tumour model after chronic oral administration at 25 mg/kg b.i.d. Compound **25**, also known as AZD8835, is currently in phase I clinical trials.

The phosphoinositide 3-kinases (PI3Ks) are a group of lipid kinases which phosphorylate the 3-hydroxyl group of phosphatidylinositol (4,5)-bisphosphate (PIP2) to phosphatidylinositol (3,4,5)-triphosphate (PIP3), while the phosphatase PTEN reverses this process.[1,2] PIP3 accumulation at the plasma membrane results in recruitment of AKT which is phosphorylated and activated, leading to a cascade of cell signalling which controls a range of cellular processes like cell proliferation, growth and survival. In mammals, there are eight PI3K family members, divided into three classes (I, II and III) based on structure, regulation and lipid substrate specificity. The PI3K Class I contains four isoforms, PI3Kα and PI3Kβ being ubiquitously expressed, whereas the expression of PI3Kδ and PI3Kγ is mainly restricted to the immune system. All four isoforms are heterodimers comprising a p110α, p110β and p110δ (Class IA) or p110γ (Class IB) catalytic subunit (for PI3Kα, PI3Kβ, PI3Kδ and PI3Kγ respectively) together with a regulatory subunit. Class IA and the Class IB are respectively activated by receptor tyrosine kinases and G-protein coupled receptors.[3-5]

The PI3K/AKT/m-TOR pathway is very commonly activated in a wide range of human cancers as a result of hyperactivation of upstream growth factor signalling, mutations, or loss of tumour suppressor genes such as PTEN.[6] Amplification and mutation of the *PIK3CA* gene encoding the p110α catalytic unit occurs frequently in common human cancers, including ca. 25% of breast cancers.[7,8] The three most common mutations (E542K, E545K and H1047R) in the *PIK3CA* gene have been confirmed as activating mutations, whilst activating mutations have not been reported for p110δ, and have only very recently been reported for p110β.[9] The strong evidence pointing at the oncogenic nature of the *PIK3CA* gene mutations and their high frequency have fuelled a strong interest in developing selective inhibitors of PI3Kα.[10,11]

The first PI3K inhibitors in clinical trials have been pan-PI3K inhibitors, inhibiting multiple PI3K isoforms.[12,13] The main concern associated with the pan-PI3K inhibitors has been their tolerability profile due to the inhibition of different PI3K enzymes. Moreover, some of the early pan-PI3K clinical candidates also have off-targets activity, especially on other members of the PI3K-related kinase (PIKK) family.[14] On the other hand, isoform-selective PI3K inhibitors may offer potential strategies for maximising the therapeutic window with added potential for combination, while eliminating the more deleterious effects which may arise from pan-isoform inhibition.[15]

At the start of this work, very few isoform-selective PI3K inhibitors exhibiting appropriate drug-like properties had been described. Idelalisib (also known as GS-1101 and CAL-101; launched in 2014) was the first isoform selective compound entering clinical trial for the treatment of cancers and, based on its selective PI3Kδ pharmacology, was developed in hematological malignancies.[16,17] More isoform selective agents are in the clinical phase, including PI3Kα isoform selective inhibitor NVP-BYL719,[18,19] PI3Kβ-sparing inhibitor GDC-0032,[20] PI3Kβ isoform selective inhibitors GSK263771[21] and SAR260301,[22] and finally dual PI3Kβ/δ inhibitor AZD8186[23] (Figure 1).

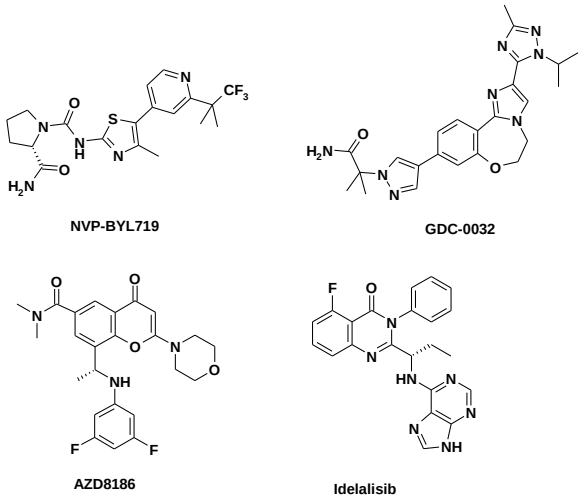

Figure 1. Structure of selected isoform selective PI3K inhibitors.

We previously reported the identification of a promising novel series of PI3K inhibitors selective for PI3Kα versus PI3Kβ and having excellent general protein kinase selectivity (exemplified by compound **3**), by designing out undesired protein kinase activity associated with our initial aminopyrazine lead while keeping the selectivity for PI3Kα versus PI3Kβ.[24] An essential aspect of that work was to improve overall general kinase selectivity from the notoriously promiscuous aminopyrazine core. During our hit identification activities, we had also identified a series of 3-oxadiazolyl-2-aminopyridines, exemplified by **1**, as potent inhibitors of PI3Kα both at the enzyme and the cellular level (Figure 2). Further exploration of the substitution on the oxadiazole identified the *tert*-butyl analogue **2** showing increased potency for PI3Kα. However, as anticipated from the similarity of this series to our initial aminopyrazine lead, aminopyridines **1** and **2** displayed poor general kinase selectivity. Again, the identity of some of those anti-targets and their known pharmacological effects might lead to an unacceptable safety profile.

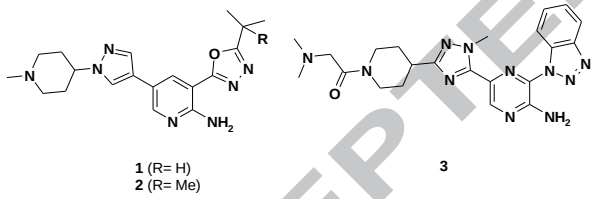

Figure 2. Structure of compounds **1**-**3**.

In this Letter, we describe the optimisation work from **1** and **2**, building potency against PI3Kα and selectivity versus PI3Kβ and more generally versus the anti-targets such as KDR, Aurora B, FGFR1 and GSK3β as surrogates of general protein kinase selectivity. Selectivity across the PI3K isoforms was routinely measured with biochemical enzyme assays and the α/β selectivity was also monitored in cell assays (inhibition of AKT phosphorylation at Thr308 in *PIK3CA* mutant human breast ductal carcinoma BT474 cells, sensitive to PI3Kα inhibition, and at Ser473 in PTEN-null breast adenocarcinoma MDA-MB-468 cells, sensitive to PI3Kβ inhibition; providing measurements of PI3Kα and PI3Kβ inhibition respectively).[23] Kinase promiscuity was routinely measured using several kinase enzyme assays: KDR, Aurora B, FGFR1, GSK3β, but for simplicity, only the KDR and/or FGFR1 enzyme results are reported in this paper. Broader kinase selectivity was confirmed for prioritized compound(s) using additional panel screens.

Compound **1-2**, **4-25** were made according to Schemes 1-3:

Suzuki coupling of commercially available **1a** with known boronic ester **26**[25] followed by functional group manipulation afforded ester **1b**, which was converted into oxadiazole **1** in three steps. Alternatively, starting from **2a**, the oxadiazole group was first assembled in the synthesis, followed by bromination of the aminopyridine, to give **2b**. Coupling of **2b** with **26**, followed by further functional group manipulation gave **2**. Compound **4** was made from previously described **4a**.[24] Synthesis of **5** is based on the key stannane **5a**, which was prepared from **2b** in two steps. Stille coupling of **5a** with dibromotriazole **27**,[24] followed by Suzuki coupling with boronic ester **28**[24] and reduction of the double bond, provided the Boc-protected desired regioisomeric triazole, which was then readily converted to **5** (Scheme 1).

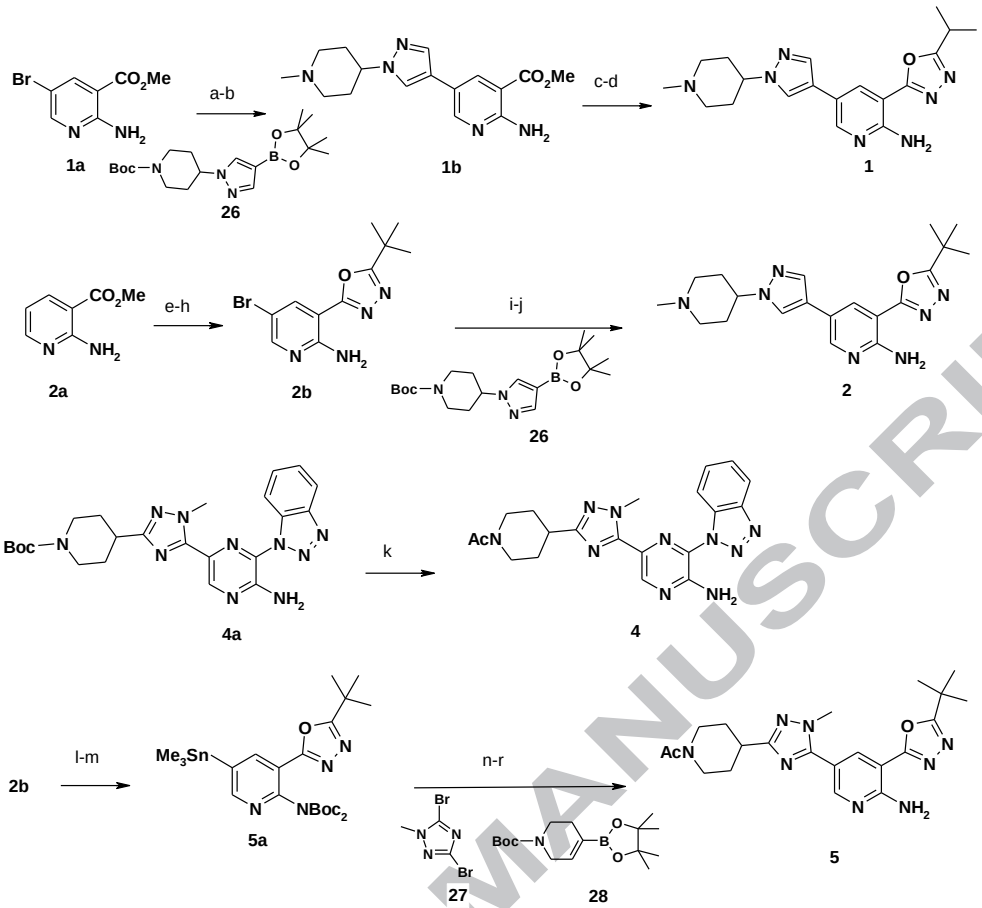

Scheme 1. Synthesis of compounds **1**, **2**, **4** and **5**. Reagents and conditions: (a) **26**, $Pd(PPh_3)_4$, Cs_2CO_3, dioxane-water (4:1), 80 °C, 2 h, 70%; (b) 4N HCl, dioxane, rt, 4 h; CH_2O, NEt^iPr_2, $NaBH(OAc)_3$, MeOH, rt, 21 h, 55%; (c) NH_2NH_2. H_2O, EtOH, 80 °C, 5 h, 94%; (d) HATU, $^iPrCO_2H$, NEt^iPr_2, NMP, rt, 48 h; P_2O_5 (1 eq.), $MeSO_3H$, 70 °C, 18 h, 4%; (e) NH_2NH_2. H_2O, EtOH, 90 °C, 15 h, 96%; (f) $^tBuCO_2H$, EDCI, HOPO, DMF, rt, 15 h, 73%; (g) ^iPr-N=C=N-^iPr, DMA, 130 °C, 4 h, 76%; (h) NBS, THF, rt, 2 h, 88%; (i) **26**, $(PPh_3)_2PdCl_2$, CsF, MeOH, 120 °C (μwave), 30 min, then TFA, rt, 67%; (j) CH_2O, $NaBH(OAc)_3$, CH_2Cl_2-MeOH (1:1), 25 °C, 10 min, 43%; (k) TFA-CH_2Cl_2 (1:1), rt, 1 h, 84%; AcCl, NEt^iPr_2, CH_2Cl_2, rt, 2 h, 85%; (l) DMAP, NEt^iPr_2, Boc_2O, DMF, rt, 60 h, 75%; (m) Sn_2Me_6, $Pd(PPh_3)_4$, toluene, 110 °C, 2 h, 66%; (n) **27**, $(PPh_3)_2PdCl_2$, LiCl, DME, 130-140 °C (μwave), 58%; (o) **28**, $(PPh_3)_2PdCl_2$, CsF, MeOH, 140 °C (μwave), 70 min, 68%; (p) Pd, HCO_2NH_4, DMF, 70 °C, 3 h, 59%; (q) TFA, CH_2Cl_2, rt, 1 h, 90%; (r) AcCl, NEt_3, CH_2Cl_2, 0 °C, 1 h, 72%.

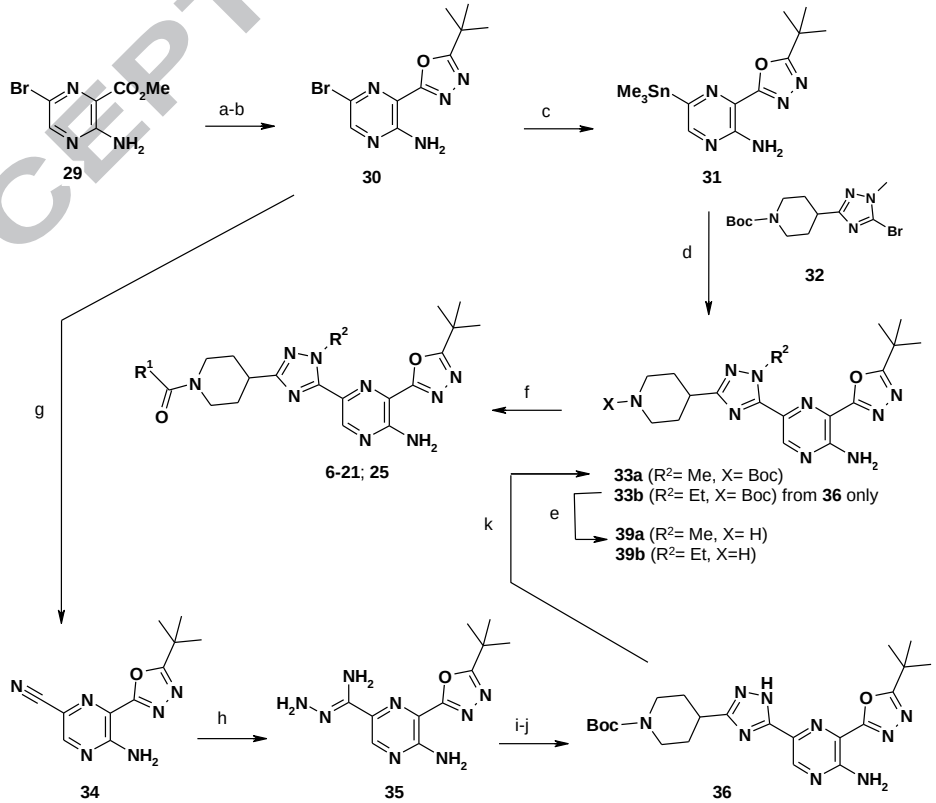

Scheme 2. Synthesis of compounds **6-21** and **25**. Reagents and conditions: (a) NH_2NH_2. H_2O, EtOH, 50 °C, 40 h, quant.; (b) $(^tBuCO)_2O$, MeCN, 80 °C, 1 h, 96%; NEt^iPr_2, TsCl (1.2 eq.), MeCN, 70 °C, 2 h, quant.; (c) Sn_2Me_6, $(PPh_3)_2PdCl_2$, toluene, 80 °C, 2 h, 39% ; (d) **32**, $(PPh_3)_2PdCl_2$, LiCl, 4-Me-2-pentanol, 140 °C, 2 h, 79% (for **33a**, R^2= Me); (e) TFA - CH_2Cl_2 (1:1), rt, quantitative; (f) THP-$OCH_2CH_2CO_2H$, HATU, NEt^iPr_2, MeCN, rt, 1 h, 97% (for **10**) and quant. (for **25**), then PPTS, MeOH, 60 °C, 90 min, 78% (for **10)** and 85% (for **25**); or AcCl, NEt^iPr_2, CH_2Cl_2, (for **6-7**); or $AcOCH_2COCl$, NEt_3, CH_2Cl_2, then aq. LiOH, MeOH (for **8**); or R^3CO_2H, EDCI, HOPO, CH_2Cl_2 or NMP (for **9**, **15**); or R^3CO_2H, NEt^iPr_2, TBTU, DMF or NMP (for **11-14**, **16-21**); (g) $Pd_2(dba)_3$ (0.025 eq), dicyclohexyl(2',4',6'-triisopropylbiphenyl-2-yl)phosphine (0.1 eq), Zn (0.1 eq), $ZnCN_2$ (0.6 eq), DMA, 100 °C, 1 h, 95% ; (h) NH_2NH_2. H_2O, ^iPrOH, 50 °C, 16 h, 79% ; (i) N-BOC isonipecotic acid, HATU, N-Me morpholine, DMA, rt, 95%; (j) AcOH, dioxane, 70-100 °C, 18 h, 77%; (k) DBU, MeI, 2-methylTHF, rt, 76% (for **33a**, R^2= Me) or DBU, EtI, 2-methylTHF, 35 °C, 80% (for **33b**, R^2= Et).

Compound **6-21** and **25** were made from compounds **33a** or **33b** by Boc deprotection followed by coupling with the corresponding carboxylic acid (Scheme 2). For hydroxyl containing side chains, protection with an acetyl (for **8**) or with a tetrahydropyranyl (for compounds **10** and **25**) was used during the amide coupling. Two routes to compound **33a** were developed, both starting from commercially available methyl 2-amino-5-bromopyrazine-2-carboxylate **29**. Ester conversion into the *tert*-butyl oxadiazole afforded the key common intermediate **30**. The first synthesis relied on the conversion of **30** into the stannane **31** using stoichiometric amounts of hexamethyldistannane, followed by Stille coupling with previously described **32**[24] to give **33a**. Therefore, a second route better suited for larger scale synthesis was developed, avoiding use of toxic tin derivatives or by-products. The bromo derivative **30** was converted into the nitrile **34** using zinc dicyanide and palladium catalysis. Addition of hydrazine onto **34** gave **35**. Coupling with N-Boc isonipecotic acid, followed by cyclisation under acidic conditions gave the key triazole **36**. Finally, regioselective methylation with methyl iodide and DBU gave **33a** in excellent yield. The ethyl analogue **33b** was obtained from **36** by reaction with ethyl iodide under similar conditions.

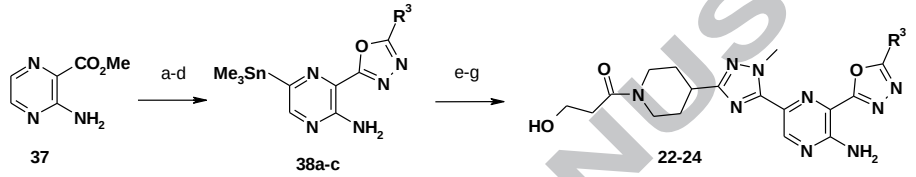

Scheme 3. Synthesis of compounds **22-24**. Reagents and conditions: (a) NH_2NH_2. H_2O, EtOH, 60 °C, 2 h, 97%; (b) R^3CO_2H, TBTU, NEt^iPr_2, MeCN, 80 °C, 20 min; NEt^iPr_2, TsCl (1 eq.), 0 °C - reflux 45-64%; (c) NBS, THF, rt, 16 h, 79-88%; (d) Sn_2Me_6, $(PPh_3)_2PdCl_2$, dioxane, 80 °C, 47-64%; (e) **32**, $(PPh_3)_2PdCl_2$, LiCl, DME, 130 °C (μwave), 36-54%; (f) TFA, rt, 30 min, 88-100%; (g) THP-$OCH_2CH_2CO_2H$, EDCI, HOPO, CH_2Cl_2, rt, 2 h; PPTS, MeOH, 60 °C, 3 h, 47-61%.

A variation on the first synthesis of the aminopyrazines was developed for the variation of the *tert*-butyl group on the oxadiazole (Scheme 3). Starting from methyl 2-aminopyrazine-2-carboxylate **37**, hydrazide formation followed by coupling with the corresponding carboxylic acid and cyclisation afforded the oxadiazoles **38a-c**. Bromination followed by stannylation and Stille coupling with **32** gave the Boc-protected derivatives. Boc deprotection, followed by amide coupling with 3-(tetrahydropyran-2-yloxy)propanoic acid[26] and final deprotection with PPTS in methanol, afforded compounds **22-24**.

Table 1.
Structure, PI3K, KDR and FGFR1 enzyme and PI3K cell inhibitory potencies of compounds **1-6**.

Cpd	substituent	Structure	PI3Kα enz. IC_{50}[a]	PI3Kβ enz. IC_{50}[a]	KDR enz. IC_{50}[a]	FGFR1 enz. IC_{50}[a]	PI3Kα cell IC_{50}[a]	PI3Kβ cell IC_{50}[a]
1	R^3 = ^{i}Pr	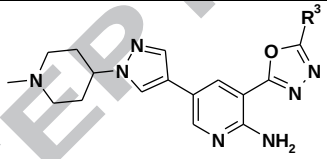	0.100	5.7	0.13	0.49	0.200	13
2	R^3 = ^{t}Bu		0.014	3.1	0.079	0.15	0.074	5.3
3	R^1CO = Me_2NCH_2CO	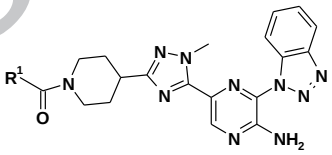	0.029	1	9.0	10	0.27	6.9
4	R^1CO = Ac		0.028	1.4	8.6[b]	17[b]	0.79	20
5	A = CH	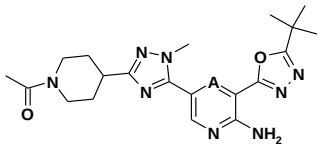	0.410	24	83[b]	>100[b]	7.6	>30[b]
6	A = N		0.068	9.6	>100[b]	>100[b]	1.0	>30

[a] Geometric means of at least two IC_{50} determinations per compound, μM.
[b] n=1.

We previously reported[24] the identification of **3** as a selective PI3Kα inhibitor versus PI3Kβ having excellent general kinase selectivity (Figure 2). We showed that replacement of the pyrazole group on the left hand side of the molecule (present in the initial lead) by the 1-methyl-1,2,4-triazole group (present in **3**) dramatically increased general kinase selectivity. However, one shortcoming identified with **3** was poor oral exposure in rat (AUC: 0.7 μM.h following an oral dose of 5 mg/kg in rat, bioavailability 10%). One possible explanation is the modest permeability measured in Caco-2 ($P_{app, A-B}$ 1.6 x 10^{-6} cm/s) associated with efflux potential (efflux ratio of 47 in the MDR-

1 overexpressing mdck cell line), probably linked to the overall low lipophilicity of **3** ($logD_{7.4}$ 0.9) in conjunction with high molecular weight and the presence of a basic side chain.[27] The neutral acetamide **4** had much higher permeability and was less prone to efflux (Caco-2 $P_{app,\ A-B}$ 36 x 10^{-6} cm/s; efflux ratio of 5 in the MDR-1 overexpressing mdck cell line). **4** retained good general kinase selectivity, but unfortunately showed a significant reduction of potency (see Table 1).

Docking of compound **2** in the publicly available crystal structure[28] of PI3Kα was performed manually, based on the binding mode of aminopyrazine and aminopyridine derivatives observed in various in-house kinase crystal structures (unpublished results). In this model (see Figure 3), **2** makes a double donor/acceptor interaction with the hinge residues Val851 and Glu849 and the sp2 nitrogen of the pyrazole ring is located at H-bond distance of the Gln859 residue that is unique to the PI3Kα isoform. This binding mode is very similar to the proposed binding mode of **3**, where one nitrogen of the triazole interacts with Gln859.[24] During the course of this work, another group reported that hydrogen bond interactions with the Gln859 side chain also was the structural determinant for PI3Kα selectivity in their aminothiazole series.[18]

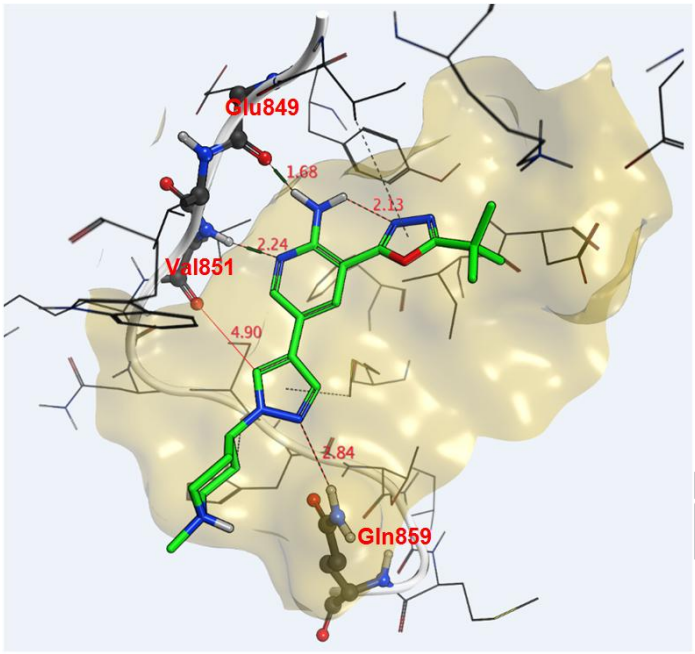

Figure 3. Compound **2** docked into the publicly available crystal structure[27] of PI3Kα.

Therefore, we thought we could apply the same strategy to solve the general kinase selectivity issue seen with **2**. But to our surprise, pyridine **5** lost most of its PI3Kα activity. Although it is difficult to fully rationalise it, we cannot exclude subtle conformational differences between the pyridine and the pyrazine cores. Indeed, we were pleased to see that the corresponding pyrazine **6** regained some potency against PI3Kα, whilst it lost activity against the two anti-targets KDR and FGFR1. The PI3Kα cell activity was still modest, but again improvement of general kinase selectivity was confirmed in a panel of kinases (see Figure 4, compound **6** vs. compound **2**). Compound **6** displayed excellent selectivity on PI3Kα vs. PI3Kβ, good physical and metabolic properties (low lipophilicity: $LogD_{7.4}$ 2.1; high permeability: Caco-2 $P_{app,\ A-B}$ 39 x 10^{-6} cm/s; low rate of metabolic turnover: rat hepatocyte and human microsomal Cl_{int}: 4.4 µL/min/10^6cell and 9 µL/min/mg, respectively; low human plasma protein binding: fraction unbound f_u 32%), but the overall PI3Kα potency would need to be improved.

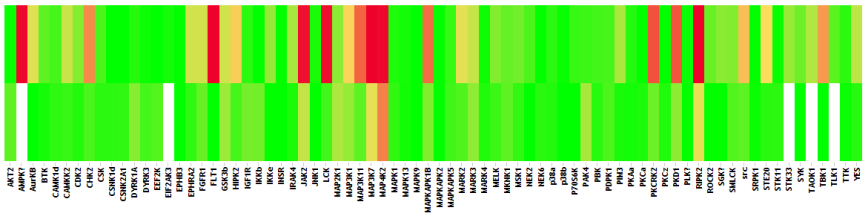

Figure 4. Heatmap showing the inhibitory activity of compound **2** (on top) and compound **6** (below) against a panel of protein kinases ('Dundee University protein kinase panel') at 1 µM. The percentage of inhibition is colored from green (0%) to yellow (60%) and red (90%).

Table 2 illustrates the modifications we explored to further optimize compound **6**. General kinase selectivity remained excellent for compounds **7**-**24**, as illustrated by the very modest KDR activity reported in Table 2 for these compounds, and will not be discussed further. Variation of the substitution on the triazole showed a significant potency change, with ethyl **7** being more potent than methyl **6**. But metabolic stability in human microsomes was also reduced, probably linked to increased lipophilicity. We then looked at the modification of the amide. Larger amides than acetamide **6** were tolerated, either linear such as **9** or **11,** or cyclic such as **12** or **13**. But again metabolic stability was an issue; some hydroxyl containing amides, such as **8** or **10**, showed acceptable metabolic stability, but others, such as **14** or to a lesser degree **15**, did not. Increasing the size of the amide (**9**-**13**) also increased PI3Kα potency. Overall, **10** showed the combination of potency, selectivity, metabolic stability we were looking for (see Table 2). However, one immediate concern was the potential β-elimination of the hydroxyl group, leading to the reactive acrylamide. To test this, we performed chemical stability measurements in aqueous conditions and trapping experiments with glutathione in human liver microsomes and did not see any evidence of formation of the acrylamide. Instead, one of the metabolites we identified in rodent, dog and human hepatocytes was the carboxylic acid resulting from oxidation of the primary alcohol, and chemical stability measurements showed traces of ring opening of the oxadiazole in aqueous solution at very acidic pH, i.e. pH 1. Because of the serious issues that formation of the acrylamide in humans would cause, we nevertheless tried to block potential β-elimination (compounds **16**-**18)**, but again poor metabolic stability was an issue, although it is worth noting that the cyclopropyl **18** was the most metabolically stable of the three. Compounds **19**-**21**, containing an extra methyl on the amide portion compared to **10** showed good potency and/or microsome stability. But overall, the 3-hydroxypropanamide present in **10** was considered as the best amide.

Table 2.
Structure, PI3K enzyme and cell inhibitory potencies and other properties of compounds **6**-**25**.

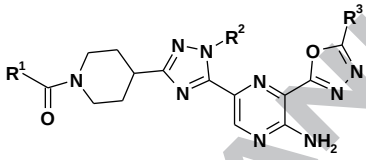

Compound	R^1	R^2	R^3	PI3Kα enz. IC_{50}[a]	PI3Kβ enz. IC_{50}[a]	KDR enz. IC_{50}[b]	PI3Kα cell IC_{50}[a]	PI3Kβ cell IC_{50}[a]	HLM Cl_{int}[c]	$LogD_{7.4}$[d]
6	Me	Me	^{t}Bu	0.068	9.6	>100	1.0	>30	9.4	2.1
7	Me	Et	^{t}Bu	0.008	0.95	10	0.22	7	25	2.5
8	CH_2OH	Me	^{t}Bu	0.045	10	47	1.1	27	4	1.4
9	CH_2OMe	Me	^{t}Bu	0.031	1.9	30	0.37	14	25	1.8
10	CH_2CH_2OH	Me	^{t}Bu	0.023	2.2	20	0.34	13	3	1.5
11	CH_2CH_2OMe	Me	^{t}Bu	0.034	3.5	26	0.26	24	35	2.1
12	4-tetrahydropyranyl	Me	^{t}Bu	0.025	2.1	20	0.4	7.8[e]	53	-
13	^{c}Pr	Me	^{t}Bu	0.022	2.6	24	0.4	15	46	-
14		Me	^{t}Bu	0.011	19[e]	51	0.62	19[e]	29	-
15	$C(Me)_2OH$	Me	^{t}Bu	0.037	6.3	24	0.42	17	13	-
16	$CH_2C(Me)_2OH$	Me	^{t}Bu	0.046	4.8	18	0.35	15	21	-
17	$C(Me)_2CH_2OH$	Me	^{t}Bu	0.032	3.4	27	0.32	16	60	-
18	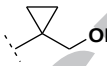	Me	^{t}Bu	0.031	2.2	26	0.41	15	11	-
19	(*R*)-$CH(Me)CH_2OH$	Me	^{t}Bu	0.032	3.4	24	0.53	24	3.5	1.8
20	(*R*)-$CH_2CH(Me)OH$	Me	^{t}Bu	0.025	2.9	25	0.31	21	13	1.8
21	(*S*)-$CH_2CH(Me)OH$	Me	^{t}Bu	0.030	3.3	20	0.27	15	10	1.8
22	CH_2CH_2OH	Me		0.024	2.5	3.3	0.42	16	4	1.4
23	CH_2CH_2OH	Me		0.102	8.1	47	1.2	>30	5.5	1.1
24	CH_2CH_2OH	Me	^{i}Pr	0.074	7.1	29	0.77	24	4.9	1.2
25	CH_2CH_2OH	Et	^{t}Bu	0.0062	0.431	6.4	0.057	3.5	8.7	1.9

[a] μM; unless stated otherwise, geometric means of at least two IC_{50} determinations per compound.
[b] μM; single IC_{50} determination or geometric means of at least two IC_{50} determinations per compound.
[c] human liver microsome intrinsic clearance (HLM Cl_{int}); $\mu L.min^{-1}.mg^{-1}$.
[d] Measured using shake-flask methodology with a buffer:octanol volume ratio of 100:1.
[e] n=1 value.

Next, we turned our attention to the oxadiazole. We considered potential replacement of the oxadiazole by other 5-membered heteroaromatics. But the proposed binding mode of these compounds in PI3Kα suggests that both nitrogens of the oxadiazole are necessary, one making an internal hydrogen bond with the aminopyrazine and maintaining some degree of planarity, and the second being involved in a H-bond acceptor, presumably with Asp933 via a water molecule, in a similar fashion as the 4-pyridine of NVP-

BYL719 interacts with PI3Kα.[18] We considered the substitution on the oxadiazole, but other groups were at best equivalent to the ^{t}Bu (i.e. **22**), with less lipophilic groups being less potent (i.e. **23** or **24**).
Finally combining the SAR elements of the different portions (best amide, substitution on the oxadiazole and the triazole) gave the increased potency we were looking for. Compound **25** displayed superior PI3Kα potency, yet with good selectivity and metabolic stability, and was selected for further profiling.

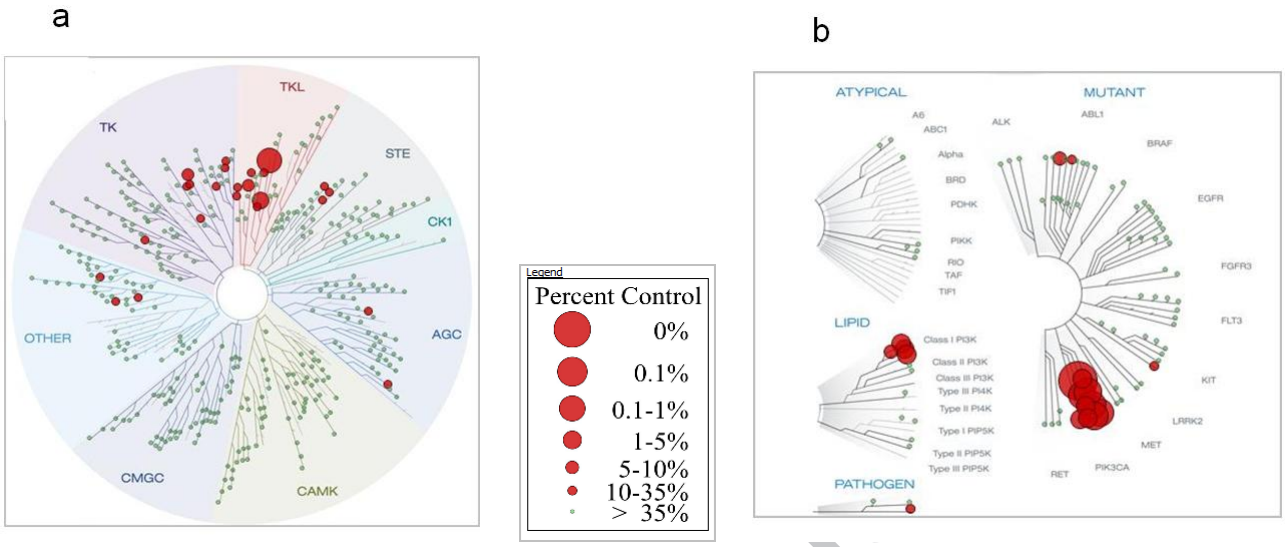

Figure 5. Kinase selectivity of compound **25** (KINOMEScan™, DiscoveRx); percentage of control at 1 μM against a panel of 456 kinases (picture a); against atypical kinases, including lipid kinases and mutant kinases (picture b).

The broader kinase selectivity of **25** was evaluated in several panels of kinase assays. **25** showed very limited activity in a panel of 71 protein kinases ('Dundee University protein kinase' panel) when tested at 1 μM, with only one kinase, GCK (germinal center kinase), showing >70% inhibition. The kinase selectivity of **25** was confirmed in the commercial KINOMEscan (DiscoveRx) against a panel of 456 kinases, where it showed no or limited competitive binding at 1 μM on the majority of the kinases (see Figure 5). The 22 kinases out of the 456 tested, where probe binding was determined to be significant at 1 μM, were further investigated. K_d determination on those 22 kinases confirmed the high degree of kinase selectivity of **25**, with only one other enzyme (ALK6, also known as BMPR1B) outside PI3K class I enzymes being within 10 fold of PI3Kα wild type (Table 10 in Supplementary data). It is worth noting that **25** showed similar potency on the mutated PI3Kα enzymes (E542K, E545K and H1047R) when compared to wild type PI3Kα enzyme. Confirmation of selectivity among the lipid kinases was assessed in a panel of 15 kinases ('Dundee University lipid kinase' panel), where an IC_{50} below 1 μM was seen for only two kinases outside PI3K class I enzymes, i.e. PI4Kα and PI4Kβ, but with more than 50 fold selectivity margin vs. PI3Kα (Table 9 in Supplementary data). Bespoke kinase assays confirmed selectivity against selected kinases from the closely related PIKK family (m-TOR IC_{50} 12.1 μM, DNAPK IC_{50} 4.0 μM). **25** was screened for inhibition of other members of the PIKK family, ATR and ATM, in cell based assays. Very weak inhibitory activity was observed against ATM (endpoint: phosphorylation of ATM at Ser1981 in HT29 cells, IC_{50} >30 μM) or ATR (endpoint: phosphorylation of Chk-1 at Ser345 in HT29 cells, IC_{50} >21 μM), consistent with the desired target selectivity profile of **25**.

Table 3
Class I PI3K kinase enzyme and cell inhibition of compound **25.**

Assay details			IC_{50} (μM)[a]
Enzyme inhibition	Class I PI3K enzyme	PI3Kα	0.0062
		Mutated PI3Kα – E545K	0.0060
		Mutated PI3Kα – H1047R	0.0058
		PI3Kβ	0.431
		PI3Kδ	0.0057
		PI3Kγ	0.090
Cellular inhibition p-AKT endpoint	PI3Kα	BT474	0.057
	PI3Kβ	MDA-MB-468	3.5
	PI3Kδ	Jeko-1	0.049
	PI3Kγ	RAW264	0.53

[a] Geometric means of multiple IC_{50} determinations.

The selectivity profile of **25** among the class I PI3K isoforms was tested in enzyme and cell based assays (Table 3). At the enzyme level, **25** is a potent mixed inhibitor of PI3Kα (IC_{50} 0.0062 μM) and PI3Kδ (IC_{50} 0.0057 μM), with selectivity against PI3Kβ (IC_{50} 0.431 μM) and PI3Kγ (IC_{50} 0.090 μM). **25** is also a potent inhibitor of the commonly occurring PI3Kα mutants, PI3Kα - E545K (IC_{50} 0.0060 μM) and PI3Kα - H1047R (IC_{50} 0.0058 μM). In cell-based assays assessing the ability to inhibit AKT phosphorylation, **25** was a potent inhibitor in cells sensitive to PI3Kα inhibition (IC_{50} 0.057 μM in *PIK3CA* mutant human breast ductal carcinoma BT474 cell line) and in cells sensitive to PI3Kδ inhibition (IC_{50} 0.049 μM in Jeko-1 B cell line), but not to cells sensitive to PI3Kβ inhibition (IC_{50}

3.5 μM in PTEN null breast adenocarcinoma MDA-MB-468 cells) or to PI3Kγ inhibition (IC_{50} 0.53 μM in monocytic RAW264 cell line).

Table 4
Physical, pharmacokinetic and other properties of compound **25**.

Properties	Value
Plasma protein binding Hu / Rat / Dog / Mo: f_u (%)[a]	14 ; 24 ; 26; 17
Intrinsic Clearance in hepatocytes, rat / dog / hu: Cl_{int} (μL/min/10^6 cell)[b]	8.6 ; < 3.4 ; < 2.0
Rat / Dog Pharmacokinetic parameters	
Clearance: Cl (mL/min/kg)[c]	11.6 / 6.7
Volume of distribution: V_d (L/kg)[c]	1.1 / 2.1
Bioavailability: F (%)[c]	47 / 96
Aqueous solubility (μM)[d]	196
Permeability Caco-2: $P_{app, A-B}$ (10^{-6} cm/s)[e]	39
CYP inhibition – 1A2, 2C9, 2C19, 2D6, 3A4 IC_{50} (μM)[f]	>30 (all)
hERG (% inhibition at 100 μM)[g]	37.9

[a] Protein binding in human, rat, dog and mouse plasma, fraction unbound f_u.
[b] Intrinsic clearance measured from fresh rat/dog hepatocytes and cryopreserved human hepatocytes, Cl_{int}.
[c] From plasma concentrations in male Han Wistar rats (at least n=2), compound administered at 4 μmol/kg i.v. and 10 μmol/kg p.o. for **25** as a formulation in HPMC/Tween for the oral arm and as a solution formulation in 10% DMA , 90% Captisol (30% w/v in water) for the iv arm; from plasma concentrations in Beagle dogs (at least n=2), compound administered orally at a dose around 2 μmol/kg as a formulation in 0.5% (w/v) HPMC, 0.1% (w/v) Tween 80 in water and i.v. at a dose around 2 μmol/kg as a solution in 5% (v/v) DMSO, 35% (v/v) tetraethylene glycol, 60% (v/v) citrate buffer. Intravenous parameters calculated from an intravenous bolus; bioavailability, from oral and i.v. AUC.
[d] Solubility in aqueous phosphate buffer, pH 6.8; from crystalline material.
[e] Permeability in Caco-2 cell line, A pH 6.5, B pH 7.4.
[f] Inhibition of cytochrome P450, IC_{50}.
[g] Inhibition of hERG potassium channel, % inhibition at 100 μM

Compound **25** displayed good solubility, good permeability and low turnover in hepatocytes from various species. As expected from the *in vitro* data, low *in vivo* clearance associated with high bioavailability was seen in both rat and dog (Table 4). Compound **25** showed high exposure following oral administration to SCID mice (AUC: 137 μM.h and c_{max} 34 μM at 50 mg/kg p.o.) and was selected for further *in vivo* evaluation.
In a pharmacodynamic experiment following chronic oral dosing (25 mg/kg b.i.d. or 6 mg/kg b.i.d. of **25**) in nude mice bearing mutant H1047R PI3Kα SKOV-3 tumour xenografts, target modulation was assessed by measuring AKT phosphorylation levels at Ser473 at 30 minutes and 8 hours. At both doses, strong inhibition of AKT phosphorylation was observed at the 30 minute timepoint. At 8 hours, significant inhibition was still seen at the 25 mg/kg dose, whereas no inhibition was seen at the lower dose of 6 mg/kg, consistent with the lower plasma concentrations observed (see Figure 6).

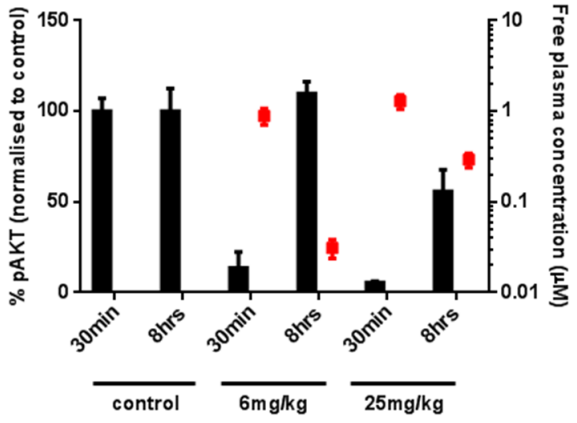

Figure 6. Inhibition of AKT phosphorylation (black bars) in the SKOV-3 xenograft model in nude mice following chronic oral administration of **25** (25 mg/kg b.i.d. and 6 mg/kg b.i.d.) and associated free plasma levels (red squares) at 30 minutes and 8 hours.

The antitumour activity of **25** was evaluated in the same model following chronic oral dosing at the same doses of 25 mg/kg b.i.d. and 6 mg/kg b.i.d. (Figure 7). Near complete inhibition of tumour growth (93% tumour growth inhibition) was seen at 25 mg/kg b.i.d., whilst the lower dose of 6 mg/kg b.i.d gave only partial inhibition of tumour growth (32% tumour growth inhibition), again consistent with the reduced inhibition of AKT phosphorylation observed 8 hours after the lower dose.
In summary, starting from a series of 2-aminopyridines exemplified by **1** and **2** as potent inhibitors of PI3Kα both at the enzymatic and the cellular level, but having modest general kinase selectivity, optimisation of this series led to the identification of the clinical candidate **25**, a potent inhibitor of PI3Kα (wild type, E545K and H1047R mutations) and PI3Kδ, selective vs. PI3Kβ and PI3Kγ, and with excellent general kinase selectivity. Compound **25** displayed low metabolic turnover and suitable physical properties for oral administration. *In vivo*, compound **25** showed pharmacodynamic modulation of AKT phosphorylation in a SKOV-3 xenograft tumour model (H1047R mutant PI3Kα) grown in mouse, after chronic oral administration at 25 mg/kg b.i.d. at the 30 minute and 8 hour timepoints. Compound **25** showed near complete inhibition of tumour growth (93% tumour growth inhibition) in the same model after chronic oral administration at 25 mg/kg b.i.d. Compound **25** (also known as AZD8835) was selected as a clinical candidate for the

treatment of *PIK3CA*-dependent cancers and is currently in phase I clinical trials. Further in vitro and in vivo biological characterization of **25** will be reported in due course.[29]

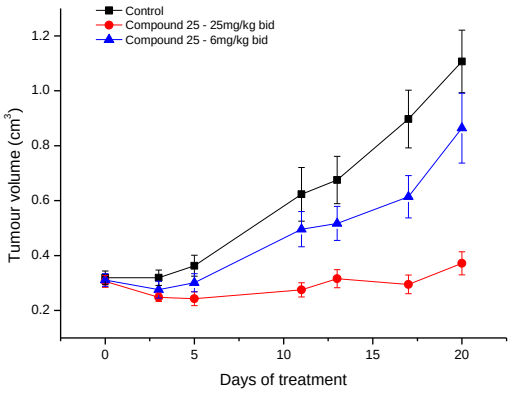

Figure 7. Tumour growth inhibition in the SKOV-3 xenograft model in nude mice following chronic oral administration of **25** (25 mg/kg b.i.d. and 6 mg/kg b.i.d.).

Acknowledgments

We acknowledge the excellent technical expertise of the scientists at AstraZeneca in particular: Vanessa Gonnot, Patrice Koza, Jonathan Lecoq, Fabrice Renaud, Gordon Currie and Stuart Wells for synthesis of compounds; Paul Davey, Christian Delvare, Delphine Dorison Duval for characterization of compounds; the members of the SAR Screening Groups for generating the cell and biochemical data; Neil James, Dan Owen, Samantha Waite nee Johnston and Cath Trigwell for biological evaluation.

Supplementary data

Supplementary data (synthetic procedures and characterization for all compounds, biological protocols and procedures for determination of physiochemical and DMPK properties) associated with this article can be found in the on-line version.

References and notes

1. Vanhaesebroeck, B.; Leevers, S. J.; Ahmadi, K.; Timms, J.; Katso, R.; Driscoll, P. C.; Woscholski, R.; Parker, P. J.; Waterfield, M. D. *Annu. Rev. Biochem.* **2001**, *70*, 535.
2. Engelman, J. A.; Luo, J.; Cantley, L. C. *Nat. Rev. Genet.* **2006**, *7*, 606.
3. Cantley, L. C. *Science* **2002**, *296*, 1655.
4. Foster, F. M.; Traer, C. J.; Abraham, S. M.; Fry, M. J. *J. Cell Sci.* **2003**, *116*, 3037.
5. Vanhaesebroeck, B.; Guillermet-Guibert, J.; Graupera, M.; Bilanges, B. *Nat. Rev. Mol. Cell. Biol.* **2010**, 11, 329.
6. Liu, P.; Cheng, H.; Roberts, T. M.; Zhao, J. J. *Nat. Rev. Drug Discov.* **2009**, *8*, 627.
7. Bachman, K. E.; Argani, P.; Samuels, Y.; Silliman, N.; Ptak, J.; Szabo, S.; Konishi, H.; Karakas, B.; Blair, B. G.; Lin, C.; Peters, B. A.; Velculescu, V. E., Park, B. H. *Cancer Biol. Ther.* **2004**, *3*, 776.
8. Wu, G.; Xing, M.; Mambo, E.; Huang, X.; Liu, X.; Guo, Z.; Chaterjee, A.; Goldenberg, D.; Gollin, S. M.; Sukumar, S.; Trink, B.; Sidransky, D. *Breast Cancer Res.* **2005**, *7*, R609.
9. Choi, M. R.; Yoo, N. J.; An, C. H.; Lee, S. H. *Human Pathology* **2015**, *46*, 753.
10. Denny, W. A. *Expert Opin. Ther. Pat.* **2013**, *7*, 789.
11. Lee J. Y.; Engelman, J. A., Cantley L. C. *Science* **2007**, 317, 206.
12. Liu, P.; Cheng, H.; Roberts, T. M.; Zhao, J. J. *Nat. Rev. Drug Discov.* **2009**, *8*, 627.
13. Courtney, K. D.; Ryan, B.; Engelman, J. A. *J. Clin. Oncol.* **2010**, *28*, 1075.
14. Fruman, D.A.; Rommel, C. *Nat. Rev. Drug Discov.* **2014**, *13*, 140.
15. Thorpe, L. M.; Yuzugullu, H.; Zhao, J. J. *Nat. Rev. Cancer* **2015**, *15*, 7.
16. Lannutti, B. J.; Meadows, S. A.; Herman, S. E. M.; Kashishian, A.; Steiner, B.; Johnson, A. J.; Byrd, J. C.; Tyner, J. W.; Loriaux, M. M.; Deininger, M.; Druker, B. J.; Puri, K. D.; Ulrich, R. G.; Giese, N. A. *Blood* **2011**, *117*, 591.
17. Norman, P. *Expert Opin. Ther. Pat.* **2011**, *11*, 1773.
18. Furet, P.; Guagnano, V.; Fairhurst, R.A.; Imbach-Weese, P.; Bruce, I.; Knapp, M.; Fritsch, C.; Blasco, F.; Blanz, J.; Aichholz, R.; Hamon, J.; Fabbro, D.; Caravatti, G. *Bioorg. Med. Chem. Lett.* **2013**, *23*, 3741.
19. Fritsch, C.; Huang, A.; Chatenay-Rivauday, C.; Schnell, C.; Reddy, A.; Liu, M.; Kauffmann, A.; Guthy, D.; Erdmann, D.; De Pover, A.; Furet, P.; Gao, H.; Ferretti, S.; Wang, Y.; Trappe, J.; Bracmann, S. M.; Sauveur-Michel M.; Wilson, C.; Boehm, M.; Garcia-Etcheverria, C.; Chene, P.; Wiesmann, M.; Cozens, R.; Lehar, J.; Schlegel, R.; Caravatti, G.; Hofmann, F.; Sellers, W. R. *Mol. Cancer Ther.* **2014**, *13*, 1117.
20. Ndubaku, C. O.; Heffron, T. P.; Staben, S. T.; Baumgardner, M.; Blaquiere, N.; Erin Bradley, E.; Bull, R.; Do, S.; Dotson, J.; Dudley, D.; Edgar, K. A.; Friedman, L.S.; Goldsmith, R.; Heald, R.A.; Kolesnikov, A.; Lee, L.; Lewis, C.; Nannini, M.; Nonomiya, J.; Pang, J.; Price, S.; Prior, W.W.; Salphati, L.; Sideris, S.; Wallin, J. J.; Wang, L.; Wei, B.; Sampath, D.; Olivero, A. G. *J. Med. Chem.* **2013**, *56*, 4597.
21. a) Blackman, S. C.; Gainer, S. D.; Suttle, B. B.; Skordos, K.W.; Greshock, J. D.; Motwani, M.; Roadcap, L. T.; Hardwicke, M. A. A.; Wooster, R. F. 103rd Ann. Meet. Am. Assoc. Cancer Res. (AACR) 2012, Abst 1752; b) A phase I/IIa, first time in human, study of GSK2636771 in subjects with advanced solid tumors with phosphatase and tensin homolog (PTEN) deficiency (NCT01458067) ClinicalTrials.gov Web Site 2011, October 20.
22. Certal, V.; Carry, J. C.; Halley, F.; Virone-Oddos, A.; Thompson, F.; Filoche-Romme, B.; Al-Ahmad, Y.; Karlsson, A.; Charrier, V.; Delorme, C.; Rak, A.; Abecassis, P.-Y.; Amara., C.; Vincent, L.; Bonnevaux, H.; Nicolas, J.-P.; Mathieu, M.; Bertrand, T.; Marquette, J. P.; Michot, N.; Benard, T.; Perrin, M.-A.; Lemaitre, O.; Guerif, S.; Perron, S.; Monget, S.; Gruss-Leleu, F.; Doerflinger, G.; Guizani, H.; Brollo, M.; Delvarre, L.; Bertin, L.; Richepin, P.; Loyau, V.; Garcia-Echeverria, C.; Lengauer, C.; Schio, L. *J. Med. Chem.* **2014**, *57*, 903.

23. Barlaam, B.; Cosulich, S.; Degorce, S.; Fitzek, M.; Green, S.; Hancox, U.; Lambert-van der Brempt, C.; Lohmann, J.-J.; Maudet, M.; Morgentin, R.; Pasquet, M.-J.; Péru, A.; Plé, P.; Saleh, T.; Vautier, M.; Walker, M.; Ward, L.; Warin, N. *J. Med. Chem.* **2015**, *58*, 943.
24. Barlaam, B.; Cosulich, S.; Fitzek, M.; Green, S.; Harris, C. S.; Hudson, K.; Lambert-van der Brempt, C.; Ouvry, G.; Page, K.; Ruston, L.; Ward, L.; Delouvrié, B. *Bioorg. Med. Chem. Lett.* **2015**, *25*, 2679.
25. de Koning, P. D.; McAndrew, D.; Moore, R.; Moses, I. B.; Boyles, D. C.; Kissick, K.; Stanchina, C. L.; Cuthbertson, T.; Kamatani, A.; Rahman, L.; Rodriguez, R.; Urbina, A.; Sandoval, A.; Rose, P. R. *Org. Proc. Res. Dev.* **2011**, *15*, 1018.
26. Barlaam, B. C.; Delouvrie, B.; Ouvry, G.; Lambert-Van der Brempt, C. M. P.; Harris, C. S.; Berry, D.; Tomkinson, G. P.; Reid, G. P. *U.S. Pat. Appl.* (2014), US 20140206700.
27. Gleeson, M. P. *J. Med. Chem.* **2008**, *51*, 817.
28. Mandelker, D.; Gabelli, S. B; Schmidt-Kittler, O.; Zhu, J.; Cheong, I.; Huang, C. H.; Kinzler, K. W.; Vogelstein, B.; Amzel, L. M. *Proc. Natl. Acad. Sci. USA* **2009**, *106*, 16996. The publicly available crystal structure of PI3Kα in complex with wortmannin was used to dock compound **2** (PBD ID code: 3HHM; coordinates available).
29. Hudson, K; Hancox, U.; Trigwell, C.; McEwen, R.; Polanska, U.; Nikolaou, M; Morentin Gutierrez, P.; Avivar-Valderas, A.; Delpuech, O.; Dudley, P.; Hanson, L.; Ellston, R.; Jones, A.; Cumberbatch, M.; Cosulich, S.; Ward, L.; Cruzalegui, F.; Green S. Intermittent high dose scheduling of AZD8835, a novel selective inhibitor of PI3Kα and PI3Kδ demonstrates treatment strategies for *PIK3CA*-dependent breast cancers. Submitted for publication.

Graphical Abstract

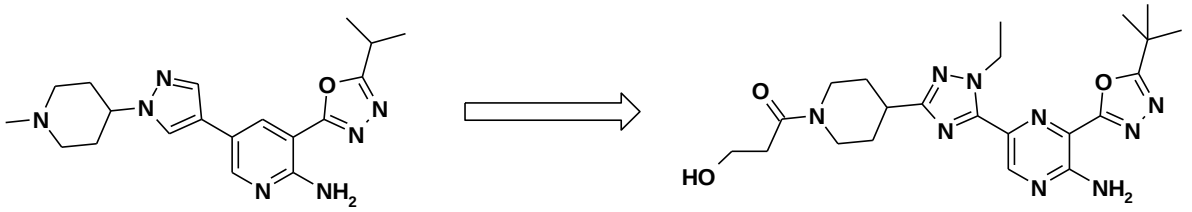

1
PI3Kα enz. IC_{50} 0.100 μM
PI3Kα cell IC_{50} 0.200 μM
poor kinase selectivity

25
PI3Kα enz. IC_{50} 0.0062 μM
PI3Kα cell IC_{50} 0.057 μM
PI3Kβ cell IC_{50} 3.5 μM
PI3Kγ cell IC_{50} 0.53 μM
PI3Kδ cell IC_{50} 0.049 μM
excellent kinase selectivity and physical properties